A NOVEL TECHNIQUE FOR BROADBAND CIRCULAR POLARIZED PIFA AND DIVERSITY PIFA SYSTEMS

Xiao-Zheng Lai[1, *], Ze-Ming Xie[2], Xuan-Liang Cen[2], and Zhi-Yong Zheng[2]

[1]School of Computer Science & Engineering, South China University of Technology, Guangzhou 510006, China

[2]School of Electronic & Information, South China University of Technology, Guangzhou 510641, China

Abstract—In this paper, a novel technique for planar inverted-F antenna (PIFA) with broadband circular polarization and pattern diversity is proposed. A defeated ground structure (DGS) has achieved broadband circular polarized (CP) PIFA by using a square branch at the ground corner with arrow-shaped slot. The pattern diversity PIFA system consists of two CP PIFAs placed symmetrically on the diagonal of DGS. Furthermore, the DGS improves port-to-port isolation by using another smaller square branch at the opposite ground corner. Finally, a prototype is fabricated and measured. The measured results agree well with simulation, and show 10-dB matching bandwidth of 16.3% (825–986 MHz), 3-dB axial ratio (AR) bandwidth of 15.5% (830–982 MHz), and 25-dB isolation bandwidth of 12.4% (848–968 MHz), which shows suitability for radio-frequency-identification (RFID) application.

1. INTRODUCTION

Recently, many researches have been conducted on Planar inverted-F antenna (PIFA) [1–5], since they are widely used in wireless communication systems due to advantages such as low profile, light weight, and conformal to the mounting structure. However, PIFAs are usually used for linear polarization, causing severe limitations for practical applications. Communication systems with circular polarized (CP) antenna can suppress multipath reflections, and reduce antenna orientation angle constraints between the transmitter and receiver [6].

For example in RFID system, antennas are utilized respectively at the reader and tag. CP radiation of reader antenna is preferred in order to make the identification reliable and more efficient, regardless of the physical orientation of the linearly polarized tag antenna [7]. CP microstrip antennas have been extensively studied [8–12]. Relatively, few designs are available for CP radiation using PIFA structure [13, 14].

Moreover, diversity and multiple-input multiple-output (MIMO) systems are considered for requirements of the next-generation wireless communications. In such communications, the scattering phenomenon is dominating the propagation process. Consequently, the received signals widely vary in phase and magnitude as a result of the multipath effect, and the overall system performance is strongly affected [15, 16]. Diversity and MIMO systems are seen as promising solutions, because they can potentially increase the channel capacity of system and improve the quality of communication link [17, 18]. To achieve high performance in diversity and MIMO systems, multiple antennas are integrated in a small handset, and should be highly isolated [19, 20]. Several techniques have been developed to enhance the port-to-port isolation of multiple antennas in diversity and MIMO systems: the neutralization technique [21–24], electromagnetic band-gap (EBG) elements [25, 26], and lumped circuit networks [27]. It should be noted that the above methods have too complex structures, and are not useful for mass production. The simple structure based on aperture coupled patch antenna (ACPA) [28] and PIFA [29, 30] are presented. However, the ACPA solution has good isolation of 25 dB with compact structure, but the isolation bandwidth of 11 MHz is too narrow to be used in most of communication systems. The PIFA solution has broad bandwidth from 1.1 GHz to 1.6 GHz, but poor isolation of 14 dB.

This paper presents a novel technique for circular polarized PIFA and polarization diversity of PIFA systems. Firstly, the proposed PIFA provides broadband CP radiation of 32.6% (768–1139 MHz) by using a square branch at the ground corner with arrow-shaped slot. Secondly, the excitation of two proposed PIFAs are located symmetrically on the diagonal of ground and realize dual circular polarization. Moreover, another smaller square branch is added at the opposite ground corner to achieve high isolation between two PIFAs. The proposed antenna and diversity system characteristics in terms of the impedance matching (S_{11}), isolation (S_{21}), axial ratio (AR), radiation pattern, and diversity performance are presented. The simulation was performed using Ansoft High Frequency Structure Simulator (HFSS), which uses the finite element method (FEM). Finally, the prototype of diversity PIFAs was fabricated and measured to confirm the simulation. The measured results show 10-dB matching

bandwidth of 16.3% (825–986 MHz), 3-dB AR bandwidth of 15.5% (830–982 MHz), and 25-dB isolation between two PIFA elements over bandwidth of 12.4% (848–968 MHz).

The organization of this paper is as follows. The circular polarized PIFA and diversity PIFAs design by using proposed technique are discussed in Sections 2 and 3, respectively. In Section 4, the experimental results are presented. The conclusions are drawn and detailed in Section 5.

2. CP PIFA DESIGN

The evolution of circular polarized PIFA is shown in Fig. 1, and the dimension of PIFAs are compared in Table 1. The proposed antennas use a 1.6-mm-thick FR4 substrate ($\varepsilon_r = 4.4$, $\tan\delta = 0.02$), and all the metallic components of antenna are printed on the same side of the substrate. As shown in Fig. 1(a), the proposed antenna design is started by Ant. I, according to the reference [14]. Ant. I consists of a PIFA structure and a square branch at the corner of square ground. The substrate dimension is fixed as 159 mm × 159 mm, and the square branch is placed at the ground corner nearby PIFA, with the length of 48 mm. As shown in Fig. 1(b), a further improvement is achieved, by applying an arrow-shaped slot under the square branch. In the improved Ant. II structure, the substrate dimension has been miniaturized to 135 mm × 135 mm, and the square-shaped branch has been reduced by 75%, with the length of 24 mm.
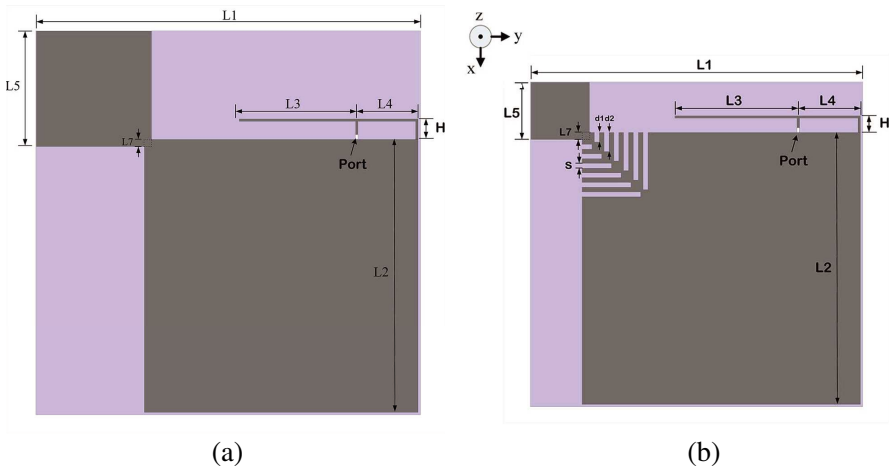

Figure 1. The evolution of CP PIFA geometry: (a) Ant. I; (b) Ant. II.

**Table 1.** Comparison of CP PIFA dimensions (unit: mm).

	L_1	L_2	L_3	L_4	L_5	L_6	L_7	H	s	$d_i, i \in (1, 6)$
Ant. I	159	114	49	24	48	/	3	8	/	/
Ant. II	135	114	49	24	24	/	3	8	2	$2 + i * 2$

In addition to size reduction of antenna, the arrow-shaped slot is still a paramount factor of the AR bandwidth. As shown in Fig. 2, the presence of arrow-shaped slot has a minor effect on the 10-dB matching bandwidth, but leads to a degradation of the 3-dB AR bandwidth. Meanwhile, the AR bandwidth of Ant. II still maintains 371 MHz (768–1139 MHz), which covers the matching bandwidth of 168 MHz (820–988 MHz). More importantly than all of that, the AR curve of Ant. II is consistent with the reflection coefficient curve. Instead, the AR curve of Ant. I is the opposite of the reflection coefficient curve. While the impedance matching performance of Ant. I becomes better, the AR response of Ant. I becomes worse, conversely.
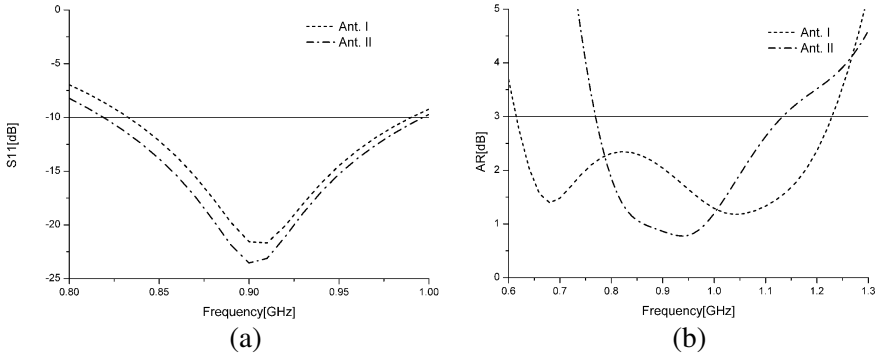

Figure 2. Arrow-shaped slot effects: (a) reflection coefficient; (b) AR.

Thus, we consider Ant. II structure as a better choice for circular polarized PIFA, which has compact size, broadband matching bandwidth of 17% (820–988 MHz) and AR bandwidth of 32.6% (768–1139 MHz). Furthermore, The parameters of Ant. II can be varied to realize optimized matching and AR bandwidth for other wireless communication systems, such as 3G/4G, and WiFi.
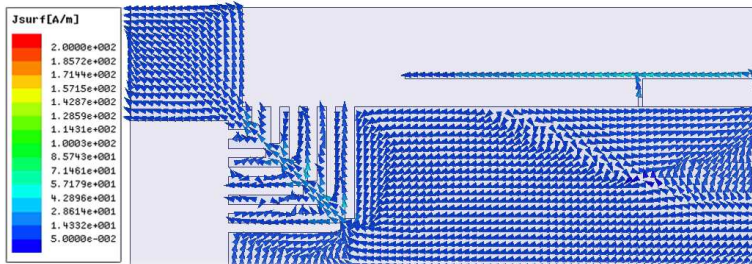
The surface current distributions on Ant. II structure at 915 MHz are shown in Fig. 3, for different time frames: $t = 0$ (0°), $T/4$ (90°), $T/2$ (180°), and $3T/4$ (270°). The current vector on ground is so weak
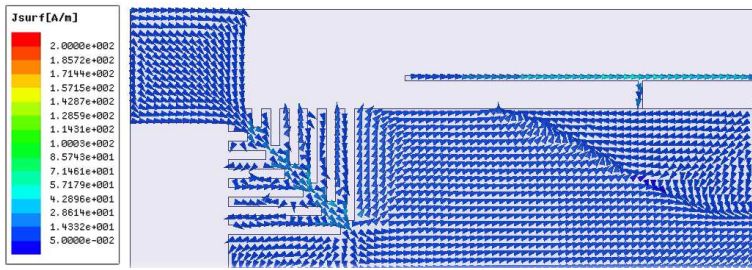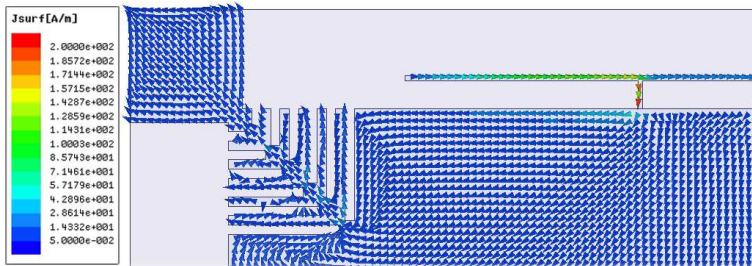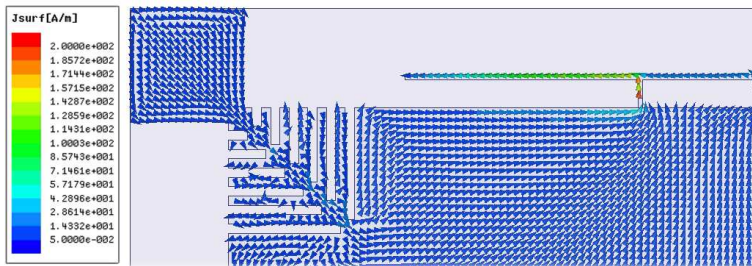
Figure 3. Surface current distribution for four different phase intervals: (a) 0°, (b) 90°, (c) 180°, (d) 270°.

that can be neglected. In Fig. 3(a), the current vector on PIFA flows downward and right, but the intensity of current flowing right is much lager than that flowing downward. Thus, when $t = 0$ (0°), the current vector on PIFA flows right. In Fig. 3(b), the intensity of current flowing downward becomes much lager than that flowing right. Thus, when $t = T/4$ (90°), the current vector on PIFA flows downward. In the same way, when $t = T/2$ (180°), the current vector on PIFA flows left, in Fig. 3(c). When $t = 3T/4$ (270°), the current vector on PIFA flows upward, in Fig. 3(d). It is stated that surface currents realize LHCP described by the tip of the current vectors (clockwise) with time. The same surface current behavior is presented throughout 700–1200 MHz, and the opposite radiation (RHCP) can be generated by symmetrical interchange of the exciting port along the diagonal of ground.

3. DIVERSITY PIFAS DESIGN

The evolution of CP diversity PIFAs is shown in Fig. 4, and the dimensions of diversity PIFAs are compared in Table 2. As shown in Fig. 4(a), Ant. III structure includes two antennas of Ant. II, which are placed symmetrically and share the same square branch and arrow-shaped slots. In order to increase the isolation between two PIFAs, the second square branch of 14 mm is applied at the ground corner opposite to the first branch, as shown in Fig. 4(b). In the improved Ant. IV structure, the substrate dimension is fixed as 149 mm × 149 mm.
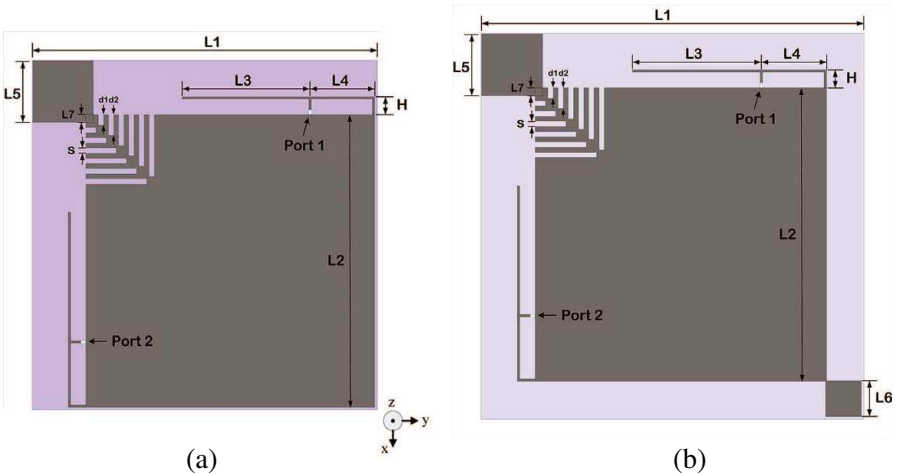

(a)   (b)

Figure 4. The evolution of CP diversity PIFAs: (a) Ant. III; (b) Ant. IV.
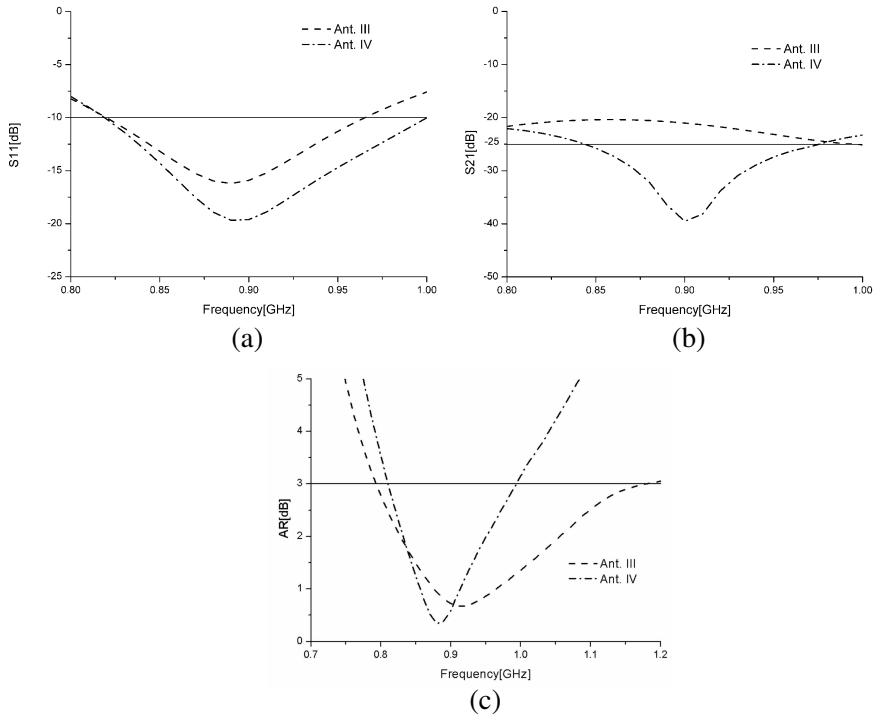
(a)

(b)

(c)

Figure 5. The second square branch effects: (a) reflection coefficient; (b) transmission coefficient; (c) AR.

Table 2. Comparison of diversity PIFAs dimensions (unit: mm).

	L_1	L_2	L_3	L_4	L_5	L_6	L_7	H	s	d_i, $i \in (1,6)$
Ant. III	135	114	49	24	24	/	3	7	2	$2 + i * 2$
Ant. IV	149	114	49	24	24	14	3	7	2	$2 + i * 2$

As shown in Fig. 5, the second square branch is a paramount factor and needs serious consideration. It is clearly observed in Figs. 5(a) and (c) that the presence of the second branch has significant improvement on the 10-dB matching bandwidth, but leads to a major degradation of the 3-dB AR bandwidth. Meanwhile, the AR bandwidth of Ant. IV still maintains 189 MHz (809–998 MHz), which covers the matching bandwidth of 172 MHz (823–995 MHz). By carefully selecting the parameter of the second branch in Ant. IV structure, a broadband 25-dB isolation bandwidth of 122 MHz (846–

968 MHz) is obtained, as shown in Fig. 5(b). On the contrary, the isolation performance of Ant. III has none bandwidth with $S_{21} \leq -25$ dB, throughout 800–1000 MHz. More importantly than all of that, the reflection coefficient, transmission coefficient and AR curves of Ant. IV structure are consistent with each other.

Thus, we consider Ant. IV structure as the proposed antenna design for diversity PIFAs system, in which simulation has broadband matching bandwidth of 17.3% (823–995 MHz), 25-dB isolation bandwidth of 12.7% (846–971 MHz) and AR bandwidth of 18.9% (809–998 MHz).

The diversity characteristic of the proposed antenna is analyzed by Simulator Ansoft HFSS ver. 13. Fig. 6 shows the simulated 3-D radiation patterns of the two PIFA feeding ports, at 915 MHz. The same radiation patterns are presented throughout 800–1000 MHz. It can be seen that the two PIFA ports have orthogonal circularized polarizations and radiation patterns, which can reduce the mutual coupling between the two PIFA elements. While port 1 exciting Left Hand Circular Polarization (LHCP) radiation at the positive Z-axis,
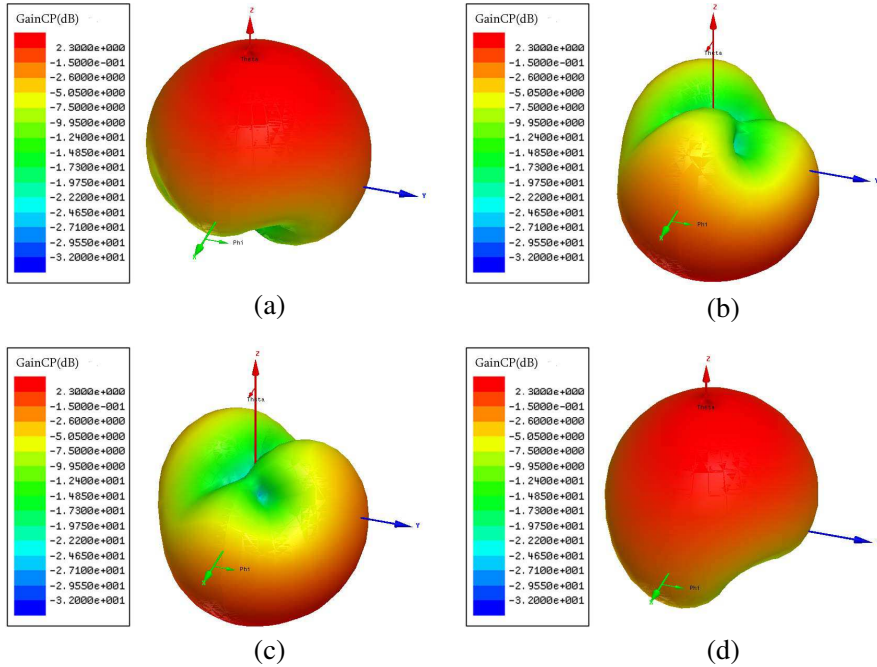

Figure 6. 3-D radiation patterns of proposed antenna at 915 MHz: (a) port 1 and (b) port2 with LHCP; (c) port1 and (d) port2 with RHCP.

port 2 generates LHCP at the negative Z-axis. Oppositely, while port 1 exciting Right Hand Circular Polarization (RHCP) radiation at the negative Z-axis, port 2 generates RHCP at the positive Z-axis. Therefore, The diversity characteristic of proposed antenna is achieved by not only orthogonal placed diversity, but also orthogonal polarizations and pattern diversity of the two PIFA elements.

4. EXPERIMENTAL RESULTS

A single layer prototype of proposed antenna is fabricated, and displayed on Fig. 7. The prototype is excited by coaxial. The outer surface of coaxial is in full conjunction with the square ground, while the inner copper is connected to the PIFA to excite the antenna. All the measured results as following are carried out in anechoic chamber using a vector network analyzer (VNA).

Figure 7. Antenna prototype view.

Compared with simulation, the measured matching and isolation bandwidths are shown in Figs. 8(a) and (b), respectively. The measured reflection coefficient magnitude ($S_{11} \leq -10$ dB) presents a matching bandwidth of 16.3% (825–986 MHz). The measured transmission coefficient magnitude ($S_{21} \leq -25$ dB) presents a bandwidth of 12.4% (848–968 MHz). Fig. 8(c) shows the measured AR response compared to the simulated results. The measured AR bandwidth ($AR \leq 3$ dB) presents a bandwidth of 15.5% (830–982 MHz). All of the above measured results are similar to simulation and totally cover ultra-high frequency (UHF) RFID band (860–960 MHz), which includes Europe Band (865–869 MHz), USA Band (902–928 MHz) and Japan Band (950–956 MHz).

The radiation patterns of prototype on port 1 at 868 MHz (middle frequency of Europe Band) are shown in Figs. 9(a) and (b). The
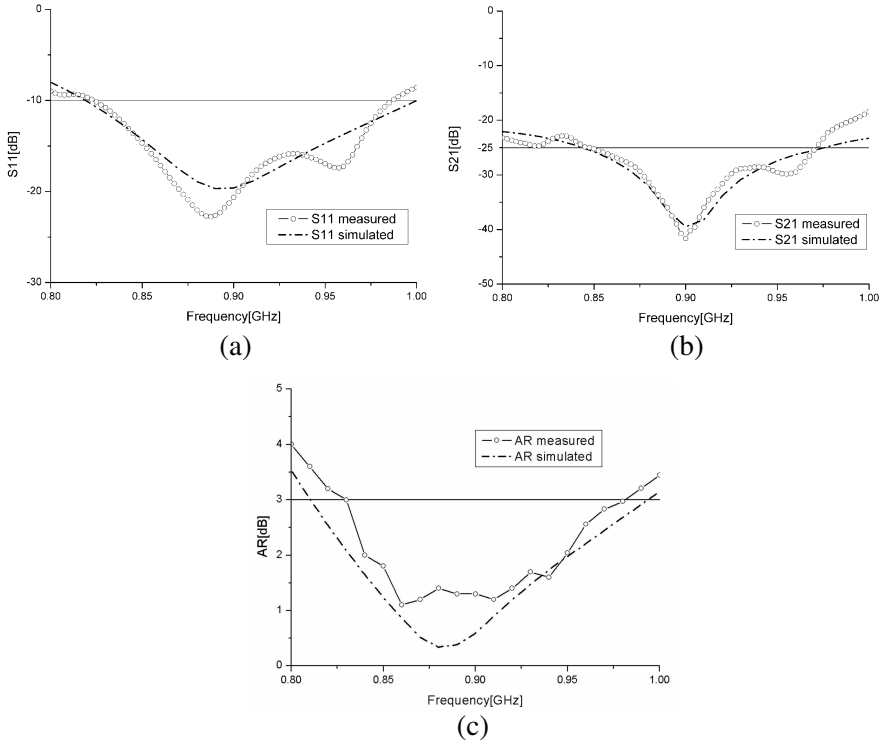
Figure 8. Antenna behavior of prototype: (a) reflection coefficient, (b) transmission coefficient, (c) AR.

corresponding results at 915 MHz (middle frequency of USA Band) are shown in Figs. 9(c) and (d), respectively. It can be seen that LHCP and RHCP radiation patterns are orthogonal in both *xoz*- and *yoz*-planes. The maximum cross-polar gain is approximately -20 dB, compared with the co-polar gains. Due to the symmetry of the prototype structure, the radiation patterns of port 2 reasonably agree with the above characteristics of port 1.

The CP gain characteristics of prototype on port 1 are shown in Fig. 10. We can find that LHCP gain curve at the positive Z-axis is similar to RHCP at the negative Z-axis. Throughout 800–1000 MHz, the gains of proposed antenna varied slightly, between 1.7 dBic and 2.3 dBic. The measured LHCP gain is 2.23 dBic at 868 MHz (Europe Band) and 2.22 dBic at 915 MHz (USA Band), which can meet the requirement for handheld RFID devices. Due to the symmetry of the prototype structure, the CP gain results of port 2 are similar to the above results of port 1.
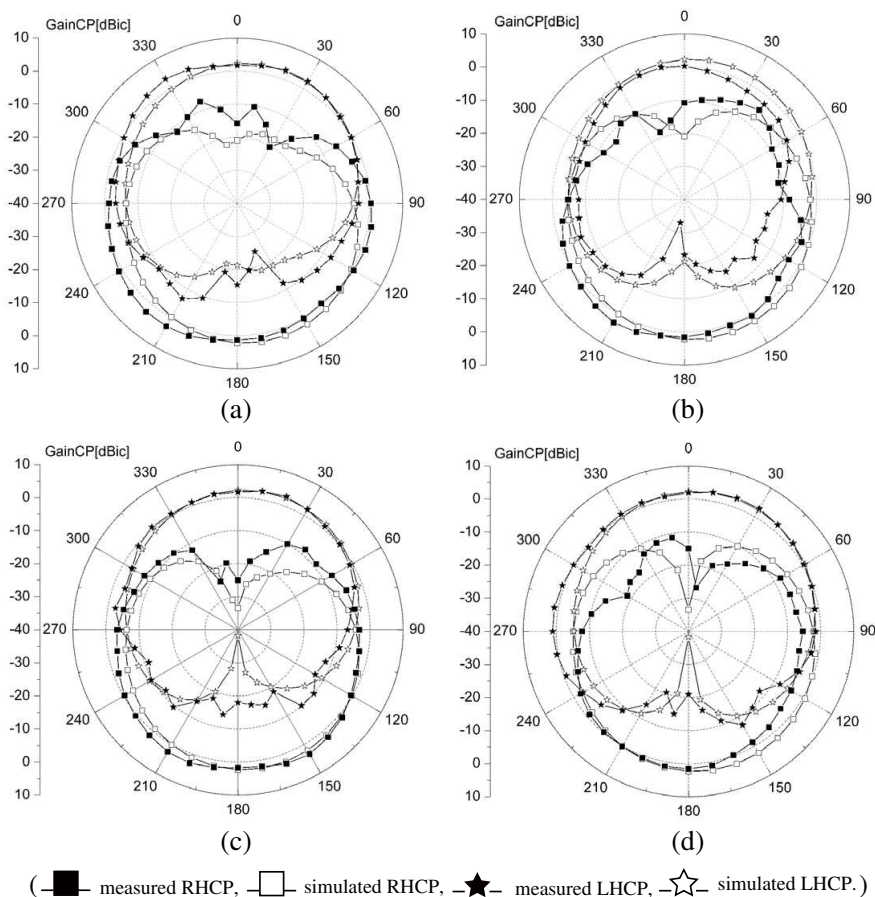
Figure 9. (a) *xoz*-plane and (b) *yoz*-plane at 868 MHz; (c) *xoz*-plane and (d) *yoz*-plane at 915 MHz.

The envelope correlation coefficient (ECC) is usually used to evaluate the diversity capability of the multi-antenna system. It should be calculated by using 3-D radiation pattern [31]. The ECC of two PIFA elements in prototype is given as following [32]:

$$\rho_{12} = \frac{|S_{11} * S_{12} + S_{12} * S_{22}|}{(1 - |S_{11}|^2 - |S_{21}|^2)(1 - |S_{21}|^2 - |S_{12}|^2)} = 0 \qquad (1)$$

The calculated ECC curve by using measured scattering parameters is presented in Fig. 11. The ECC of proposed antenna is below 0.02 from 847 MHz to 968 MHz, which leads to perfect diversity performance for UHF RFID Band (860–960 MHz).
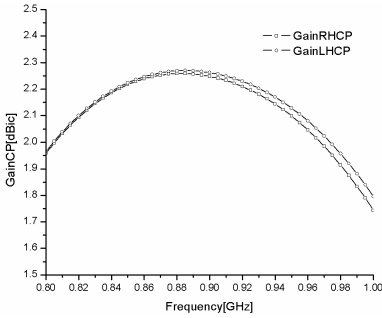
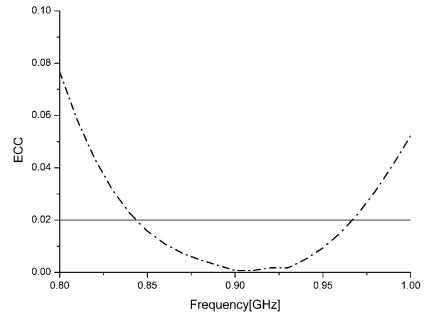**Figure 10.** Gain characteristic of prototype in port 1.

Figure 11. ECC characteristic of antenna prototype.

5. CONCLUSIONS

A novel technique for CP PIFA and polarization diversity of PIFAs system is achieved by using DGS. The CP PIFA structure uses a square branch at ground corner with arrow-shaped slot and provides broadband CP radiation characteristics of 32.6% (768–1139 MHz). In addition, the isolation between two orthogonal placed CP PIFAs is improved by another smaller square branch at the opposite ground corner. Finally, the prototype of diversity PIFAs was fabricated and measured, which showed good agreement with simulation. The measured 10-dB matching bandwidth and 3-dB AR bandwidth are 16.3% (825–986 MHz) and 15.5% (830–982 MHz), respectively. The measured 25-dB isolation bandwidth can over 12.4% (848–968 MHz). It can be concluded that The proposed technique is suitable for RFID antenna design. This technique can be used to realize circularized polarization diversity for most wireless communication systems, such as MIMO and 4G.

ACKNOWLEDGMENT

REFERENCES

1. Li, P., J. Pan, D. Yang, Z.-P. Nie, and J. Xing, "A novel quad-band (GSM850 to IEEE 802.11a) PIFA for mobile handset," *Progress In Electromagnetics Research*, Vol. 137, 539–549, 2013.

2. Soh, P. J., S. J. Boyes, G. A. E. Vandenbosch, Y. Huang, and S. L. Ooi, "On-body characterization of dual-band all-textile PIFA," *Progress In Electromagnetics Research*, Vol. 129, 517–539, 2012.

3. Lee, M.-J., Y.-S. Kim, and Y. Sung, "Frequency reconfigurable planar inverted-F antenna (PIFA) for cell-phone applications," *Progress In Electromagnetics Research C*, Vol. 32, 27–41, 2012.

4. Yu, H.-Z. and Q.-X. Chu, "A broadband PIFA with zeroth-order resonator loading," *Progress In Electromagnetics Research Letters*, Vol. 21, 67–77, 2011.

5. Wong, H., K. M. Luk, and C. H. Chan, "Small antennas in wireless communications," *Proceedings of the IEEE*, Vol. 100, 2109–2121, 2012.

6. Balanis, C. A., *Antenna Theory: Analysis and Design*, 3rd edition, Wiley, New York, 2005.

7. Finkenzeller, K., *RFID Handbook, Radio-frequency Identification Fundamentals and Applications*, 2nd edition, Wiley, New York, 2004.

8. Tsai, C.-L., "A coplanar-strip dipole antenna for broad-band circular polarization operation," *Progress In Electromagnetics Research*, Vol. 121, 141–157, 2011.

9. Rezaeieh, S. A. and M. Kartal, "A new triple band circularly polarized square slot antenna design with crooked T and F-shape strips for wireless applications," *Progress In Electromagnetics Research*, Vol. 121, 1–18, 2011.

10. Joseph, R. and T. Fukusako, "Bandwidth enhancement of circularly polarized square slot antenna," *Progress In Electromagnetics Research B*, Vol. 29, 233–250, 2011.

11. Tsai, C.-L., "A coplanar-strip dipole antenna for broadband circular polarization operation," *Progress In Electromagnetics Research*, Vol. 121, 141–157, 2011.

12. Sze, J.-Y. and S.-P. Pan, "Design of broadband circularly polarized square slot antenna with a compact size," *Progress In Electromagnetics Research*, Vol. 120, 513–533, 2011.

13. Sylvain, P., S. Robert, and K. Georges, "Planar inverted F antenna circularly polarized for RFID applications," *2012 IEEE Antennas and Propagation Society International Symposium (APSURSI)*, 1–2, Jul. 2012.

14. Wen, L. H., Y. Z. Yin, and Y. Wang, "A novel PIFA antenna for broadband circular polarization," *Microw. Opt. Technol. Lett.*, Vol. 53, 204–208, 2011.

15. Zhang, Y., Z. Ye, and C. Liu, "Estimation of fading coefficients in the presence of multipath propagation," *IEEE Trans. on Antennas and Propag.*, Vol. 57, No. 7, 2220–2224, 2009.

16. Tang, Z. and A. S. Mohan, "Characterize the indoor multipath propaga-tion for MIMO communications," *Asia-Pacific Conference Proceedings, APMC 2005*, Vol. 4, 4–7, China, Dec. 2005.

17. Gesbert, D., M. Shafi, D. S. Shiu, P. Smith, and A. Naguib, "From theory to practice: An overview of MIMO space-time coded wireless systems," *IEEE J. Sel. Areas Commun.*, Vol. 21, No. 3, 281–302, Apr. 2003.

18. Jensen, M. A. and J. W. Wallace, "A review of antennas and propagation for MIMO wireless communications," *IEEE Trans. on Antennas and Propag.*, Vol. 52, No. 11, 2810–2824, Nov. 2004.

19. Sarrazin, J., Y. Mahe, S. Avrillon, and S. Toutain, "Four co-located antennas for MIMO systems with a low mutual coupling using mode confinement," *IEEE Antennas and Propagation Society International Symposium, AP-S 2008*, 1–4, San Diego, CA, Jul. 2008.

20. Fletcher, P. N., M. Dean, and A. R. Nix, "Mutual coupling in multi-element array antennas and its influence on MIMO channel capacity," *Electron. Lett.*, Vol. 39, 342–344, Feb. 2003.

21. Diallo, A., C. Luxey, P. L. Thuc, and G. Kossiavas, "Study and reduction of the mutual coupling between two mobile phone PIFAs operating in the DCS1800 and UMTS bands," *IEEE Trans. on Antennas and Propag.*, Vol. 54, No. 11, 3063–3074, Nov. 2006.

22. Diallo, A., C. Luxey, P. L. Thuc, and G. Kossiavas, "An efficient two-port antenna-system for GSM/DCS/UMTS multi-mode mobile phones," *Electron. Lett.*, Vol. 43, No. 7, 369–370, Mar. 2007.

23. Diallo, A., C. Luxey, P. L. Thuc, R. Staraj, and G. Kossiavas, "Enhanced two-antenna structures for UMTS diversity terminals," *IET Microw., Antennas Propag.*, Vol. 2, No. 1, 93–101, Feb. 2008.

24. Luxey, C. and D. Manteuffel, "Highly-efficient multiple antennas for MIMO-systems," *2010 International Workshop on Antenna Technology (iWAT)*, 1–3, Mar. 2010.

25. Hsu, C. C., K. H. Lin, H. L. Su, and C. Y. Wu, "Design of MIMO antennas with strong isolation for portable applications," *IEEE Antennas and Propagation Society International Symposium, APSURSI'09*, 1–4, Charleston, SC, Jun. 2009.

26. Makinen, R., V. Pynttari, J. Heikkinen, and M. Kivikoski, "Improve-ment of antenna isolation in hand-held devices using

miniaturized electromagnetic band-gap structures," *Microw. Opt. Technol. Lett.*, Vol. 49, No. 10, 2508–2513, Oct. 2007.

27. Chen, S. C., Y. S. Wang, and S. J. Chung, "A decoupling technique for increasing the port isolation between two strongly coupled antennas," *IEEE Trans. on Antennas and Propag.*, Vol. 56, No. 12, 3650–3658, Dec. 2008.

28. Lai, X. Z., Z. M. Xie, and X. L. Cen, "Design of dual circularly polarized antenna with high isolation for RFID application," *Progress In Electromagnetics Research*, Vol. 139, 25–39, 2013.

29. Yao, Y., X. Wang, and X. D. Chen, "Novel diversity/MIMO PIFA antenna with broadband circular polarization for multimode satellite navigation," *IEEE Trans. on Antennas Propag. Lett.*, Vol. 11, 65–68, 2012.

30. Liu, Z. Q., Z. Qian, Z. P. Han, and W. Ni, "Design of a wideband dual circularly polarized microstrip antenna," *2012 International Conference on Microwave and Millimeter Wave Technology (ICMMT)*, Vol. 3, 1–4, 2012.

31. Salonen, I. and P. Vainikainen, "Estimation of signal correlation in antenna arrays," *Proc. 12th Int. Symp. Antennas.*, Vol. 2, 383–386, 2002.

32. Blanch, I., J. Romeu, and I. Corbella, "Exact representation of antenna system diversity performance from input parameter description," *Electron. Lett.*, Vol. 39, 705–707, 2003.